# Scattering of High-Energy Electrons by Nuclei*

A. E. GLASSGOLD†
*Department of Physics and Laboratory for Nuclear Science and Engineering, Massachusetts Institute of Technology, Cambridge, Massachusetts*

(Received February 7, 1955)

Calculations of elastic scattering of electrons have been carried out for simple, spherically symmetric charge distributions. The atomic numbers considered are $Z=13$, 29, 50, 74, and 79, and the electron energy varies from 15 to 90 Mev. The results for the homogeneous and shell distributions indicate that shape independence exists for energies such that $kR_h \lesssim 1.5$, where $R_h$ is the radius of the homogeneous model and $k$ is the electron wave number. This is a consequence of requiring that these two densities have the same mean square radius or second moment. The assumption that the scattering at higher energies depends on higher even moments has also been investigated. The scattering was calculated as a function of the fourth moment at an energy just above the shape independent region. Equating the second and fourth moments of two charge densities results in identical scattering for scattering angles up to 120°, but beyond this point the scattering differs by about 10 percent. An analysis of the existing experiments below 100 Mev indicates that the mean square radius of the nuclear charge density is given by a homogeneous distribution of radius $R_h=r_0A^{\frac{1}{3}}\times10^{-13}$ cm., with $r_0=1.2$ to within 10 percent.

## I. INTRODUCTION

RECENT experiments on elastic scattering of electrons by atomic nuclei have yielded important information about the nuclear charge distribution. The results obtained by Lyman, Hanson, and Scott[1] with 15.7-Mev electrons have been analyzed by Bitter and Feshbach[2] to indicate a radius for the nuclear charge distribution given by $r_0=1.1$ in the usual rule,

$$R=r_0A^{\frac{1}{3}}\times10^{-13}\text{ cm}. \quad (1)$$

Agreement with this value of $r_0$, which is about 20 percent smaller than the one formerly quoted, has been obtained in other electron scattering experiments by Pidd, Hammer, and Raka[3] with 33- and 43-Mev electrons and by Hofstadter's group at Stanford for energies from 84 to 183 Mev.[4,5] There is also much additional evidence[2,6] for a smaller radius, as in the measurements by Fitch and Rainwater[7] of the energy levels of $\mu$-mesonic atoms. In this paper exact numerical calculations of the elastic scattering of electrons are performed for energies from 15 to 90 Mev and the atomic numbers $Z=13$, 29, 50, 74, and 79. Some mention will also be made of the possibility of interpreting the experiments in terms of the moments of the nuclear charge density.

As a simple first approximation the nucleus is considered to be a spherically symmetric, static charge density inside a sphere of radius $R$. The interaction between the electron and the nucleus is simply the electrostatic potential between a point charge $-e$ and a charge $Ze$ distributed over a finite region. Consequently, one is dealing with the diffraction of an electron of reduced wavelength $\lambda$ by a charge distribution of linear dimension $R$. An essential parameter is the ratio of these two lengths,

$$R/\lambda=kR,$$

where $k$ is the electron wave number. For long wavelengths ($kR\ll1$) the nucleus may be treated as a point charge, but when the wavelength becomes the same order of magnitude as the radius ($kR\gtrsim1$) significant deviations from point scattering will be obtained. In the latter case the electron's energy is much greater than the rest energy. For a heavy nucleus such as gold $kR=1$ corresponds to roughly 30 Mev.

The interpretation of electron scattering experiments depends on exact solutions of the Dirac equation. Such solutions have already been given by Elton[8] and Acheson[9] for energies where only one partial wave is modified by the finite nuclear size. Calculations at much higher energies have subsequently been reported by Yennie, Ravenhall, and Wilson[10,11] and Brenner, Brown, and Elton.[12] Unfortunately the Born approximation and analogous perturbation expressions for the phase shifts are too crude except for the lightest nuclei. The failure of the Born approximation is well known for the case of point Coulomb scattering from the exact calculation by Bartlett and Watson[13] for $Z=80$ and from the higher Born approximations derived by McKinley and Feshbach.[14] For finite nuclei and an energy low enough so that the familiar oscillatory behavior of the Born approximation cross section is not

* This work was supported in part by the Office of Naval Research and the U. S. Atomic Energy Commission.

† Now at Oak Ridge National Laboratory, Oak Ridge, Tennessee.

[1] Lyman, Hanson, and Scott, Phys. Rev. **84**, 626 (1951).
[2] F. Bitter and H. Feshbach, Phys. Rev. **92**, 837 (1953).
[3] Pidd, Hammer, and Raka, Phys. Rev. **92**, 436 (1953).
[4] Hofstadter, Fechter, and McIntyre, Phys. Rev. **92**, 978 (1953).
[5] Hofstadter, Hahn, Knudsen, and McIntyre, Phys. Rev. **95**, 512 (1954).
[6] L. N. Cooper and E. M. Henley, Phys. Rev. **92**, 801 (1953).
[7] V. L. Fitch and J. Rainwater, Phys. Rev. **92**, 789 (1953).
[8] L. R. B. Elton, Proc. Phys. Soc. (London) **A63**, 1115 (1950).
[9] L. K. Acheson, Phys. Rev. **82**, 488 (1951).
[10] Yennie, Ravenhall, and Wilson, Phys. Rev. **95**, 500 (1954).
[11] D. G. Ravenhall and D. R. Yennie, Phys. Rev. **96**, 239 (1954).
[12] Brenner, Brown, and Elton, Phil. Mag. **45**, 524 (1954).
[13] J. H. Bartlett and R. E. Watson, Proc. Am. Acad. Arts Sci. **74**, 53 (1940).
[14] W. A. McKinley, Jr., and H. Feshbach, Phys. Rev. **74**, 1759 (1948).

present, Elton has compared the Born approximation with his exact calculation of the ratio of the scattering to that for a point nucleus. In this case the Born approximation gives ratios which are roughly 50 percent too large for scattering angles beyond 60°. At higher energies it has been found[10,12] that the Born approximation can be misleading in that the actual cross section decreases quite smoothly with angle as compared to the pronounced maxima and minima of the Born approximation.

Approximate methods, however, can be helpful as guides for more precise calculations. Indeed, the effect of the finite nuclear size on electron scattering was first discussed by Guth[15] and Rose[16] with the Born approximation. Another example is Feshbach's explanation of the *shape independence* of electron scattering for low energies. Acheson[9] had previously carried out exact calculations for two simple charge distributions: (1) the *homogeneous* charge distribution, in which the nuclear charge is uniformly distributed throughout the interior of a sphere of radius $R_h$; (2) the *shell* charge distribution, in which the nuclear charge is uniformly distributed over the surface of a sphere of radius $R_s$. Acheson noticed that, for the entire range of his calculation, the shell and homogeneous phase shifts were the same if the shell radius $R_s$ was about $\frac{3}{4}R_h$. Using a variational principle for the phase shift, Feshbach[17] showed that this equivalence applied more generally to any two charge densities, $\rho_1(r)$ and $\rho_2(r)$, whose mean square radii or second moments were equal:

$$\int d^3r\, r^2\rho_1(r)=\int d^3r\, r^2\rho_2(r). \tag{2}$$

For the shell and homogeneous distributions this leads to the relation,

$$R_s/R_h=(3/5)^{\frac{1}{2}}=0.775, \tag{3}$$

which agrees very closely with Acheson's exact calculations. Feshbach's restriction of this result to long wavelengths ($kR\ll 1$) can be discarded, however, since Acheson's work shows that shape independence holds at least up to $kR_h=1$. In fact, Elton[18] and Bodmer[19] have extended Feshbach's proof up to 35 or 40 Mev by applying perturbation methods directly to the Dirac radial equations.

The value of a general principle such as shape independence is that it provides a direct connection between the scattering and some essential characteristic of the nuclear charge distribution, in this case the second moment. This is especially useful in view of the difficulty of exact numerical solutions. If the general dependence of the scattering on the charge distribution is not known, special forms for the charge density must be assumed until one is found which agrees with experiment. However, this procedure may not be unique. Charge densities which are rather dissimilar in radial dependence may yet produce the same scattering, as was found for the shell and homogeneous distributions at low energies. What is needed, perhaps, is a standard set of parameters or properties of the nuclear charge density, which would apply equally well to all possible charge densities. If all these parameters were specified, the nuclear charge density would be uniquely determined as far as electron scattering was concerned. Otherwise, if only a few were known, any charge distribution which had these properties would be acceptable.

In Sec. IV we shall give some qualitative arguments for describing the scattering in terms of the even moments of the nuclear charge density. For a charge density $\rho(r)$ with a finite cutoff $R$, these are defined as

$$I^{(n)}=4\pi\int_0^R dr\, r^{n+2}\rho(r), \quad (n=0, 2, 4, \cdots). \tag{4}$$

According to the results quoted previously,[9,17–19] the scattering at low energies can be described in terms of the first two even moments, the total charge, and the mean square radius. A test of the moment interpretation at an energy just above the range of shape independence will be made in Sec. V. This involves exact calculations for charge densities slightly more complicated than the shell and homogeneous densities. The energy is such that only one additional moment, the fourth, should be effective. However, a brief summary of the calculational procedure will be first given in Sec. II. Section III will be devoted to calculations for the shell and homogeneous distributions for a wide variety of atomic numbers and energies to determine the range of shape independence. After the discussion of the effect of higher moments in Secs. IV and V, the experimental situation below 100 Mev will then be reviewed in Sec. VI.

## II. PHASE SHIFT DESCRIPTION OF ELECTRON SCATTERING

The scattering theory for the Dirac equation has been given by Mott,[20] and his notation is followed here. The wave function is expanded in partial waves characterized by the total angular momentum and parity quantum numbers $j$ and $\kappa$. Actually, Mott uses the orbital angular momentum quantum number $l$, so that for a given $j$, there are two values of $l$, $j+\frac{1}{2}$ for $\kappa=+(j+\frac{1}{2})$ states and $j-\frac{1}{2}$ for $\kappa=-(j+\frac{1}{2})$ states. If the rest mass is neglected, the phase shifts for these two states are identical[17,21] and the value of $l$ for the

[15] E. Guth, Akad. Wiss. Wien. Math.-naturw. Kl. Anz. **71**, 299 (1934).
[16] M. E. Rose, Phys. Rev. **73**, 279 (1948).
[17] H. Feshbach, Phys. Rev. **84**, 1206 (1951).
[18] L. R. B. Elton, Proc. Phys. Soc. (London) **A66**, 806 (1953).
[19] A. R. Bodmer, Proc. Phys. Soc. (London) **A66**, 1041 (1953).
[20] N. F. Mott and H. S. W. Massey, *Theory of Atomic Collisions* (Oxford University Press, London, 1949).
[21] L. K. Acheson, Ph.D. thesis, Massachusetts Institute of Technology, 1950 (unpublished).

$\kappa<0$ states is sufficient for purposes of notation,

$$j=l+\tfrac{1}{2}, \quad (l=0, 1, 2, \cdots).$$

The error in the cross section from neglect of the rest mass[12,21] is of order $(Z\alpha/k)^2$, where $\alpha$ is the fine structure constant and $k$ is the energy in units of $mc^2$.[22] For these calculations the error is always less than 1 percent.

The effect of the finite extension of the nuclear charge is described in terms of the difference $\delta_l$ between the total phase shift $\eta_l$ and the point Coulomb phase shift $\eta_l^+$

$$\delta_l=\eta_l-\eta_l^+. \tag{5}$$

These phase shifts are defined by the asymptotic form of the Dirac radial functions

$$\begin{aligned} f_l &\xrightarrow[kr\to\infty]{} k^{\frac{1}{2}}\sin(kr+Z\alpha\ln 2kr-\tfrac{1}{2}l\pi+\eta_l^+ +\delta_l), \\ g_l &\xrightarrow[kr\to\infty]{} -k^{\frac{1}{2}}\cos(kr+Z\alpha\ln 2kr-\tfrac{1}{2}l\pi+\eta_l^+ +\delta_l) \end{aligned} \tag{6}$$

and the requirement that $f_l$ and $g_l$ vanish for $r=0$. The radial functions satisfy a pair of coupled linear first-order differential equations,

$$\begin{aligned} \left(\frac{d}{dr}-\frac{l+1}{r}\right)f_l &= -(k-V)g_l, \\ \left(\frac{d}{dr}+\frac{l+1}{r}\right)g_l &= (k-V)f_l. \end{aligned} \tag{7}$$

The evaluation of the $\delta_l$ for the charge densities considered here follows closely the method used by Elton.[8] These charge densities all have a finite cut-off radius $R$, so that for $r\geq R$ the potential is Coulombic. In this region the radial functions are a linear combination of regular and irregular Coulomb functions,[23]

$$\begin{pmatrix} f_l \\ g_l \end{pmatrix}=A_l^+\begin{pmatrix} f_l^+ \\ g_l^+ \end{pmatrix}+A_l^-\begin{pmatrix} f_l^- \\ g_l^- \end{pmatrix} \quad (r\geq R). \tag{8}$$

The regular $(f_l^+, g_l^+)$ and irregular $(f_l^-, g_l^-)$ Coulomb functions are solutions of Eq. (7) with $V=-Z\alpha/r$, and have the indicial behavior $r^{\rho_{l+1}}$ and $r^{-\rho_{l+1}}$, respectively, with $\rho_{l+1}=[(l+1)^2-Z^2\alpha^2]^{\frac{1}{2}}$. The asymptotic forms of these functions are given by Eq. (6) with $\delta_l=0$, and $\eta_l^+$ replaced by $\eta_l^-$ for the irregular functions. Closed expressions for the Coulomb phase shifts have been derived by Mott.[20] By substituting the asymptotic form of each of the functions in Eq. (8), Elton obtained the following expression for the phase shift difference:

$$\tan\delta_l=\frac{\sin(\eta_l^- -\eta_l^+)}{(A_l^+/A_l^-)+\cos(\eta_l^- -\eta_l^+)}. \tag{9}$$

The ratio $A_l^+/A_l^-$ is then evaluated from Eq. (8) at $r=R$:

$$\frac{A_l^+}{A_l^-}=-\left.\frac{f_l^- -(f_l/g_l)g_l^-}{f_l^+ -(f_l/g_l)g_l^+}\right|_{r=R}. \tag{10}$$

In Eqs. (9) and (10), the ratio $f_l/g_l$ of the interior solutions is the only quantity, other than the radius $R$, which depends on the nuclear charge density. All of the others are point charge solutions. These have been collected in another report[24] which gives the methods of calculation and tables of the quantities themselves. In particular, the radial functions are evaluated from the series solutions $u_l^\pm$ and $v_l^\pm$ about the origin,

$$\begin{pmatrix} f_l^\pm \\ g_l^\pm \end{pmatrix}=B_l(kr)^{\pm\rho_{l+1}}\begin{pmatrix} u_l^\pm \\ v_l^\pm \end{pmatrix}. \tag{11}$$

With the normalization constant $B_l$ chosen to give the asymptotic forms in Eq. (6), the expression for $A_l^+/A_l^-$ in Eq. (10) becomes

$$\begin{aligned} \frac{A_l^+}{A_l^-}=-(2kR)^{-2\rho_{l+1}}&\left|\frac{\Gamma(-\rho_{l+1}+1+iZ\alpha)}{\Gamma(\rho_{l+1}+1+iZ\alpha)}\right|\frac{\Gamma(2\rho_{l+1}+1)}{\Gamma(-2\rho_{l+1}+1)} \\ &\times\left[\frac{l+1-\rho_{l+1}}{l+1+\rho_{l+1}}\right]^{\frac{1}{2}}\left[\frac{u_l^- -(f_l/g_l)v_l^-}{u_l^+ -(f_l/g_l)v_l^+}\right]_{r=R}. \end{aligned} \tag{12}$$

Finally, Acheson has shown that, for energies much greater than the rest energy, the scattering cross section may be written as

$$k^2\sigma(\theta)=|G^c+G'|^2\sec^2(\theta/2). \tag{13}$$

The function $G^c(Z\alpha,\theta)$ is the amplitude for scattering by a point charge tabulated by Feshbach,[25] and $G'(Z\alpha,kR;\theta)$ is the change in the scattering amplitude due to the finite size of the nucleus,

$$\begin{aligned} G'=\frac{1}{2i}\sum_{l=0}(l+1)&\exp(2i\eta_l^+)(e^{2i\delta_l}-1) \\ &\times[P_l(\cos\theta)+P_{l+1}(\cos\theta)]. \end{aligned} \tag{14}$$

The reason for the decomposition in Eq. (13) of the scattering amplitude is that the convergence of the series for $G'$ is much better than that for the Mott series for $G^c$ or $(G^c+G')$. The difficulties with the latter are associated with the long range of the Coulomb potential. The number of terms in Eq. (14) is only about $(kR+1)$. It is easier to do the difficult job of obtaining $G^c$ just once and to evaluate $G'$ for specific charge densities. On the other hand, there may be strong destructive interference between the two amplitudes. Then both $G^c$ and $G'$ have to be known to several more significant figures than is required for their sum.

[22] From this point, relativistic units are used in which $\hbar=m=c=1$.

[23] The plus and minus signs refer to regular and irregular, respectively.

[24] A. E. Glassgold and E. W. Mack, Massachusetts Institute of Technology Laboratory for Nuclear Science and Engineering, Technical Report No. 65, August 31, 1954 (unpublished).

[25] H. Feshbach, Phys. Rev. 88, 295 (1952).

For this reason, Yennie, Ravenhall, and Wilson[10] have devised a new method for evaluating the point Coulomb scattering amplitude $G^c$ which is more simple and more accurate than previous ones.[13,25] Their results for $Z=13$, 29, and 79 have been used here[26] and their method has been applied to the additional cases of $Z=50$ and $Z=74$.

## III. SHELL AND HOMOGENEOUS CHARGE DISTRIBUTIONS

In order to determine the range of validity of shape independence, it is sufficient to compare the simple-shell and homogeneous-charge densities used by Elton and Acheson. This is a safe comparison because the shell distribution deviates so much more widely from the homogeneous distribution than some more physically reasonable model. The shell distribution is used, of course, because of its simple radial functions.

The potentials for the shell and homogeneous distributions are square and oscillator wells, respectively:

$$V_s=-Z\alpha/R_s, \qquad (r\leq R_s); \quad (15a)$$

$$V_h=-\tfrac{1}{2}(Z\alpha/R_h)(3-r^2/R_h^2), \quad (r\leq R_h). \quad (15b)$$

The solutions of Eq. (7) for the shell distribution are spherical Bessel functions of argument $(kR_s+Z\alpha)$:

$$f_l(R)=j_l(kR_s+Z\alpha), \quad g_l(R)=j_{l+1}(kR_s+Z\alpha). \quad (16)$$

In this case $(k-V)$ is a constant and the differential equations may be identified as the recurrence relations for the spherical Bessel functions.[27] For the homogeneous distribution, series solutions about the origin are perhaps the easiest way of evaluating $f_l/g_l$:

$$f_l=r^{l+1}\sum_{n=0} a_n^{(l)}r^n \quad g_l=r^{l+1}\sum_{n=1} b_n^{(l)}r^n. \quad (17)$$

The series coefficients are obtained from the coupled recurrence relations

$$\begin{aligned} na_n^{(l)}&=-[1+\tfrac{3}{2}Z\alpha/kR_h]b_{n-1}^{(l)} \\ &\quad +[\tfrac{1}{2}Z\alpha/(kR_h)^3]b_{n-3}^{(l)}, \\ (n+2l+2)b_n^{(l)}&=[1+\tfrac{3}{2}Z\alpha/kR_h]a_{n-1}^{(l)} \\ &\quad -[\tfrac{1}{2}Z\alpha/(kR_h)^3]a_{n-3}^{(l)}. \end{aligned} \quad (18)$$

Once the ratios $f_l/g_l$ are evaluated, the analysis of the preceding section is complete. The angular distributions $k^2\sigma(\theta)$ calculated in this way are given in Figs. 1, 2, 3, 4, and 5 for the atomic numbers $Z=13$,

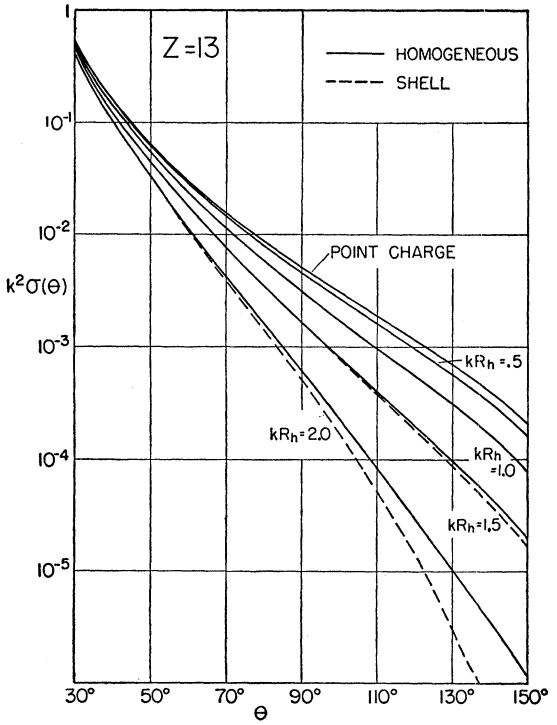


FIG. 1. Angular distributions, $k^2\sigma(\theta)$, of electrons scattered by aluminum for the homogeneous and shell distributions as a function of $kR_h$. The mean square radii of the two densities are equal $(kR_s=0.775kR_h)$. For $kR_h=0.5$ and 1.0 the models are indistinguishable on this plot. For $kR_h=1.5$ and 2.0 the dash curves are for the shell, the solid curves for the homogeneous distribution. With $r_0=1.2$, $kR_h=1.0$ corresponds to an energy of 55 Mev.

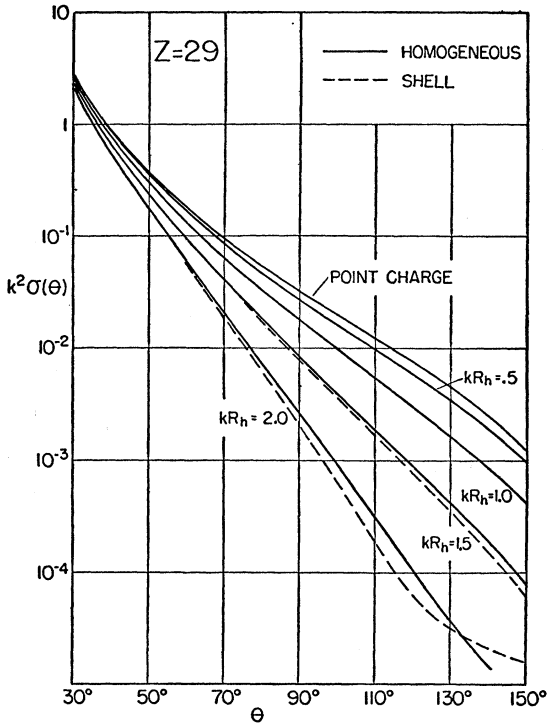


FIG. 2. Angular distributions, $k^2\sigma(\theta)$, of electrons scattered by copper for the homogeneous and shell distributions as a function of $kR_h$. The mean square radii of the two densities are equal $(kR_s=0.775kR_h)$. For $kR_h=0.5$ and 1.0 the models are indistinguishable on this plot. For $kR_h=1.5$ and 2.0 the dash curves are for the shell, the solid curves for the homogeneous distribution. With $r_0=1.2$, $kR_h=1.0$ corresponds to an energy of 41 Mev.

[26] The author would like to thank Dr. D. R. Yennie for permission to use these results before publication.

[27] P. M. Morse and H. Feshbach, *Methods of Theoretical Physics* (John Wiley and Sons, Inc., New York, 1953).

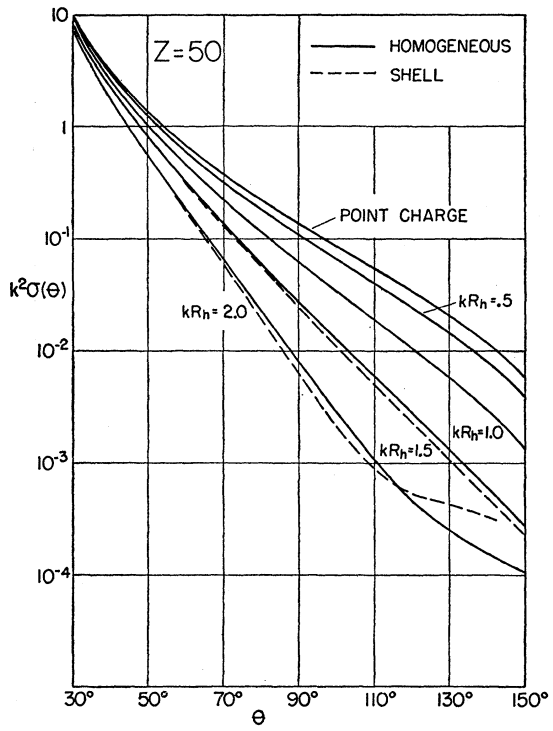


FIG. 3. Angular distributions, $k^2\sigma(\theta)$, of electrons scattered by tin for the homogeneous and shell distributions as a function of $kR_h$. The mean square radii of the two densities are equal ($kR_s=0.775kR_h$). For $kR_h=0.5$ and 1.0 the models are indistinguishable on this plot. For $kR_h=1.5$ and 2.0 the dash curves are for the shell, the solid curves for the homogeneous distribution. With $r_0=1.2$, $kR_h=1.0$ corresponds to an energy of 33 Mev.

29, 50, 74, and 79. The radii of the two charge densities have been adjusted according to Eq. (3) so that their second moments are equal. The solid curves in these figures are for the homogeneous distribution for $kR_h=0.5$, 1.0, 1.5, and 2.0. The corresponding angular distributions for the shell distribution with $kR_s=0.775\times(kR_h)=0.3875$, 0.775, 1.1625, and 1.55 are presented as dash curves only if they can be distinguished from those for the homogeneous distribution. Thus the cross sections for the shell and homogeneous distributions for $kR_h=0.5$ and 1.0 are indistinguishable on this plot, corresponding to tabular differences of a few percent. For $kR_h=1.5$ there appear small differences near 90° which increase to 10 or 15 percent at 150°. As $kR_h$ becomes larger, the differences between the angular distributions at a given angle continue to increase. If the cross section can be measured with better than 10 percent accuracy beyond 90°, then it should be possible to distinguish between charge densities for $kR_h\gtrsim1.5$. In terms of the electron's energy, the upper limit for shape independence is thus roughly 85, 65, 50, and 45 Mev for the atomic numbers $Z=13$, 29, 50, and 79, respectively.[28] This result has been verified by calculations with other charge densities, such as those discussed in Sec. V. Potentials depending on the fourth power of $r$ have also been considered.

Elton[18] and Bodmer[19] have used perturbation methods to show that shape independence of electron scattering holds outside the long wavelength region. The upper limit obtained by them is only slightly smaller than found here ($kR_h=1.5$) from exact calculations. Elton, for example, derived the following exact equation for the difference in the $l$th phase shift for the two potentials $V_1$ and $V_2$:

$$\sin[\eta_l^{(1)}-\eta_l^{(2)}]=-\frac{1}{k}\int_0^\infty dr(V_1-V_2)\times[f_l^{(1)}f_l^{(2)}+g_l^{(1)}g_l^{(2)}]. \quad (19)$$

Similar expressions have also been obtained by Parzen,[29] Rose,[30] and Elton.[31] If the phase shifts and radial functions are known for some (unperturbed) potential $V_1$, then a simple approximation for the other phase shift is obtained from Eq. (19) by using the same radial functions for $V_2$:

$$\sin[\eta_l^{(1)}-\eta_l^{(2)}]\simeq-\frac{1}{k}\int_0^\infty dr(V_1-V_2)[f_l^{(1)2}+g_l^{(1)2}]. \quad (20)$$

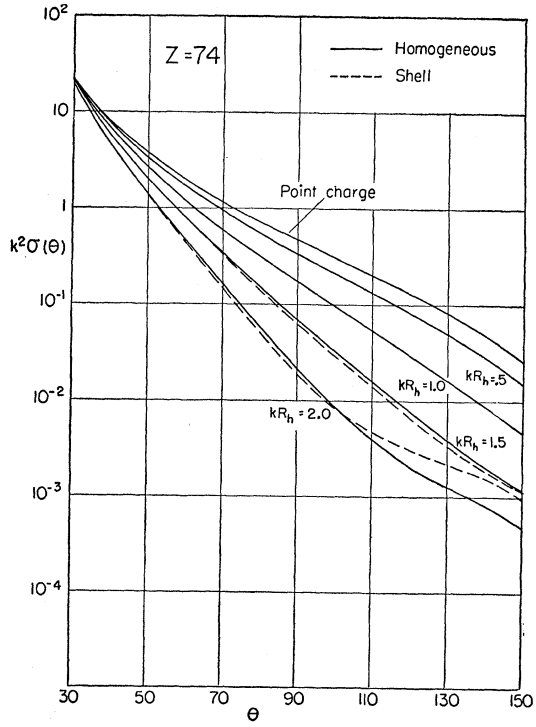


FIG. 4. Angular distributions, $k^2\sigma(\theta)$, of electrons scattered by tungsten for the homogeneous and shell distributions as a function of $kR_h$. The mean square radii of the two densities are equal ($kR_s=0.775kR_h$). For $kR_h=0.5$ and 1.0 the models are indistinguishable on this plot. For $kR_h=1.5$ and 2.0 the dash curves are for the shell, the solid curves for the homogeneous distribution. With $r_0=1.2$, $kR_h=1.0$ corresponds to an energy of 29 Mev.

[28] With $r_0=1.2$, $kR_h=1$ corresponds to electron energies of 55, 41, 33, 29, and 28 Mev for $Z=13$, 29, 50, 74, and 79, respectively.

[29] G. Parzen, Phys. Rev. **80**, 261 (1950).
[30] M. E. Rose, Phys. Rev. **82**, 389 (1951).
[31] L. R. B. Elton, Proc. Phys. Soc. (London) **A65**, 481 (1952).

We have used this method to compute homogeneous phase shifts from shell and Coulomb phase shifts. A comparison with exactly calculated phase shifts shows this approximation to be in error by about 50 percent. Better results would be expected for cases where the perturbed and unperturbed charge densities are not so different. This has been borne out by recent calculations of Trammel.[32]

## IV. INTERPRETATION OF THE SCATTERING IN TERMS OF MOMENTS

To obtain the scattering for a particular charge density the phase shift differences $\delta_l$ have to be evaluated by the methods presented in Sec. II. The phase shift differences themselves are not really convenient for describing the nuclear charge density, however, because a clear connection is lacking between individual $\delta_l$ and specific properties of $\rho(r)$. Moreover, the number of phase shift differences needed for an exact calculation is usually larger than the number of parameters obtained from the observed scattering. Thus, for $kR_h=1$, $\delta_0$ and $\delta_1$ must be evaluated although the scattering determines only the mean square radius. At higher energies Ravenhall and Yennie[11] find that

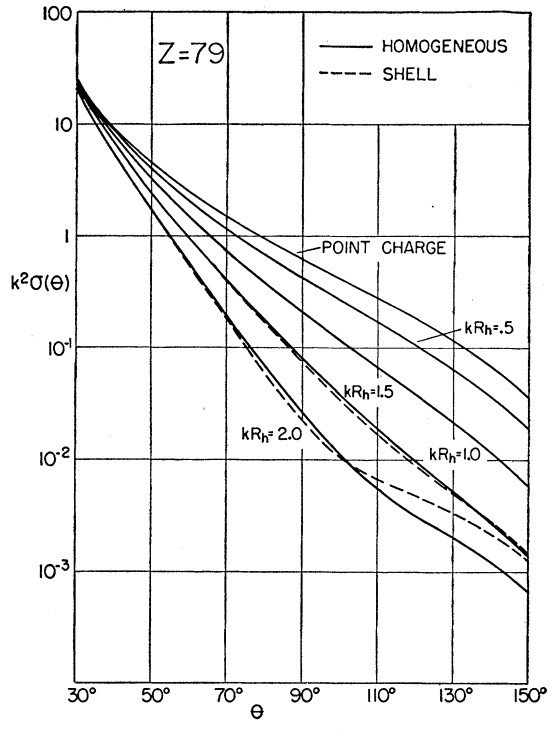


FIG. 5. Angular distributions, $k^2\sigma(\theta)$, of electrons scattered by gold for the homogeneous and shell distributions as a function of $kR_h$. The mean square radii of the two densities are equal ($kR_s=0.775kR_h$). For $kR_h=0.5$ and 1.0 the models are indistinguishable on this plot. For $kR_h=1.5$ and 2.0 the dash curves are for the shell, the solid curves for the homogeneous distribution. With $r_0=1.2$, $kR_h=1.0$ corresponds to an energy of 28 Mev.

[32] G. T. Trammel, Oak Ridge National Laboratory Semiannual Progress Report No. 1798, September 10, 1954 (unpublished).

for $kR_h=4$, where six phase-shift differences are used, only one additional parameter can be obtained from the experimental data, a "surface distance." This surface distance is defined as the distance in which the charge density decreases from its essentially constant interior value to zero. Finally, the particular form of $\rho(r)$ which gives agreement with experiment may contain more information than the observed scattering implies. This is certainly so at low energies ($kR_h<1.5$) where only the mean square radius is essential. Similarly, in the work of Ravenhall and Yennie from 84 to 183 Mev for gold, it has been found that the scattering is insensitive to details inside the surface region.

Because the amount of information which can be obtained from electron scattering is limited, it would be useful to describe the nuclear charge density in terms of some minimum set of parameters. At low energies we have used the first two even moments of the charge density, the total charge and the mean square radius. For all $Z$ and $kR_h\gtrsim1.5$, charge densities with equal zeroth and second moments are indistinguishable. It may be possible to describe the differences which occur at higher energies in terms of the higher even moments defined in Eq. (4). This is suggested by the long wavelength limit of Eq. (20) for $\delta_l$ after two integrations by parts:

$$\sin\delta_l \propto 4\pi\int_0^R drr^{2l+4}\rho(r). \tag{21}$$

Setting $l=0$ leads to Feshbach's result in Eq. (2). Certainly charge densities which are functions of only even powers of $r$ can be characterized by the even moments. Thus, just above the shape independent region, the fourth moment should also be important. If this assumption is correct, charge densities, whose first three moments ($I^{(0)}$, $I^{(2)}$, $I^{(4)}$) are equal, must give the same scattering in this energy range ($kR_h\gtrsim1.5$). To test this condition, we shall introduce in the next section charge densities with variable fourth moments. Their second moments will be set equal to that for the homogeneous distribution,

$$I^{(2)}=4\pi\int_0^R drr^4\rho(r)=\tfrac{3}{5}ZeR_h^2, \tag{22a}$$

and their fourth moments will be expressed in units of the homogeneous fourth moment,

$$I^{(4)}=4\pi\int_0^R drr^6\rho(r)=\lambda[(3/7)ZeR_h{}^4]. \tag{22b}$$

## V. DOUBLE SHELL AND n CHARGE DISTRIBUTIONS

The first charge density considered is a simple combination of the shell and homogeneous charge densities which will be referred to as the "$\eta$ distribution." A shell of charge $\eta Ze$ and radius $R_\eta$ encloses a region of constant charge density. The $\eta$ distribution is not

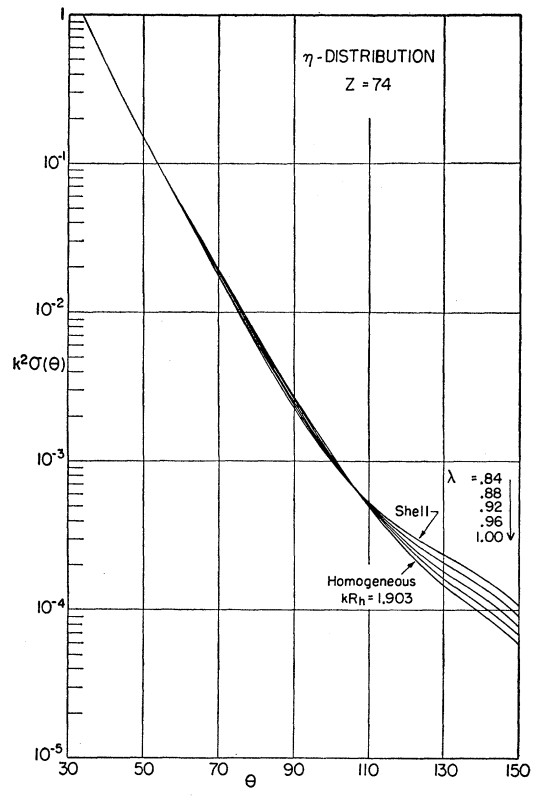


FIG. 6. Angular distributions, $k^2\sigma(\theta)$, for $\eta$-distribution for $Z=74$ and an energy of 55 Mev. This model consists of a shell, of charge $\eta Ze$ and radius $R_\eta$, enclosing a region of constant charge density; $\eta$ and $R_\eta$ are chosen so that (1) the mean square radius equals that of the homogeneous distribution with $r_0=1.2$ and (2) the fourth moment $\lambda$ assumes the values 0.84, 0.88, 0.92, 0.96, and 1.00. These parameters are listed in Table I.

completely unreasonable, for in a primitive way it represents the concentration of protons near the nuclear surface suggested by Feenberg.[33] Placing the shell at the edge, makes the potential parabolic as in the case of the homogeneous distribution in Eq. (15b),

$$V_\eta=-\tfrac{1}{2}Z\alpha[(3-\eta)-(1-\eta)r^2/R_\eta^2]/R_\eta. \quad (23)$$

The radial functions are obtained by the same series method used for the homogeneous distribution; the series coefficients in Eq. (17) are now found from the recurrence formulas

$$\begin{aligned} na_n^{(l)}&=-[1+3Z\alpha/2kR_\eta]b_{n-1}^{(l)} \\ &\quad+[Z\alpha/2(kR_\eta)^3]b_{n-3}^{(l)}, \\ (n+2l+2)b_n^{(l)}&=[1+3Z\alpha/2kR_\eta]a_{n-1}^{(l)} \\ &\quad-[Z\alpha/2(kR_\eta)^3]a_{n-3}^{(l)}. \end{aligned} \quad (24)$$

Table I lists the values of $\eta$ considered and Fig. 6 gives the calculated angular distributions for $Z=74$ and an energy corresponding to $kR_h=1.90258$. If the radius of the equivalent homogeneous charge density is given by Eq. (1) with $r_0=1.2$, then the energy is 55 Mev. The angular distributions in Fig. 6 differ only slightly up to 108° where they intersect. Beyond this, appreciable differences occur. The extreme curves are for the shell ($\eta=1, \lambda=0.84$) and homogeneous ($\eta=0, \lambda=1.00$) distributions. Equal changes in the fourth moment ($\Delta\lambda=0.04$) result in nearly equal reductions (about 15 percent) in the large-angle scattering. The scattering for angles less than 108° is characteristic of the mean square radius.

The other charge distribution considered is the "double-shell," which consists of two concentric shells of charge $Z_1e$ and $Z_2e$, and of radii $r_1$ and $r_2$, respectively ($r_1\leq r_2$). The potential inside the inner shell is a constant,

$$k-V_{ss}=k+\frac{Z_1\alpha}{r_1}+\frac{Z_2\alpha}{r_2}, \quad (r<r_1), \quad (25a)$$

so that the radial solutions are spherical Bessel functions. Between the shells, there is a $1/r$ term from the Coulomb potential of the inner shell:

$$k-V_{ss}=k+\frac{Z_1\alpha}{r}+\frac{Z_2\alpha}{r_2}, \quad (r_1<r<r_2). \quad (25b)$$

Outside both shells, the potential is Coulombic:

$$k-V_{ss}=k+\frac{Z\alpha}{r}, \quad (r>r_2). \quad (25c)$$

The radial functions for $r_1<r<r_2$ are Coulomb functions for the atomic number $Z_1$ and an energy $(k+Z_2\alpha/r_2)$. We shall choose $Z_1$ from those values for which the Coulomb functions are already tabulated in reference 24. The only complication is the additional matching point, but the phase shift differences are still given by Eqs. (9) and (10) with all quantities there evaluated for $Z=Z_1+Z_2$ and $r=r_2$. The only change is that $(f_l/g_l)_{r=r_2}$ in Eq. (10) is now

$$\left(\frac{f_l}{g_l}\right)_{r=r_2}=\frac{-(t_2/t_1)^{2\rho l+1(Z_1)}C_l(Z_1,t_1)u_l^+(Z_1,t_2)+u_l^-(Z_1,t_2)}{-(t_2/t_1)^{2\rho l+1(Z_1)}C_l(Z_1,t_1)v_l^+(Z_1,t_2)+v_l^-(Z_1,t_2)}, \quad (26)$$

TABLE I. Parameters of the $\eta$ distribution used to calculate the scattering in Fig. 6. This model consists of a shell, of charge $\eta Ze$ and radius $R_\eta$, enclosing a region of constant charge density. The energy is 55 Mev and $Z=74$; $\eta$ and $R_\eta$ are chosen to give the values of the fourth moment $\lambda$ listed below, keeping the mean square radius equal to that of the homogeneous distribution with $r_0=1.2$.

| $\eta$ | $R/R_h$ | $\lambda$ |
|---|---|---|
| 1.000 | 0.775 | 0.84 |
| 0.795 | 0.808 | 0.88 |
| 0.592 | 0.847 | 0.92 |
| 0.375 | 0.894 | 0.96 |
| 0.000 | 1.000 | 1.00 |

[33] E. Feenberg, Phys. Rev. **59**, 593 (1940).

with

$$C_l(Z_1,t_1)=\frac{u_l^-(Z_1,t_1)-(j_l/j_{l+1})_{y_1}v_l^-(Z_1,t_1)}{u_l^+(Z_1,t_1)-(j_l/j_{l+1})_{y_1}v_l^+(Z_1,t_1)},$$

where $t_1=kr_1+Z_2\alpha(r_1/r_2)$, $y_1=t_1+Z_1\alpha$, $t_2=kr_2+Z_2\alpha$. With $Z_1=50$, and $Z=74$, $r_1$ and $r_2$ are chosen so that Eq. (22) is satisfied and the fourth moment ranges from $\lambda=0.84$ to $\lambda=1.16$ in steps of 0.04. The various parameters associated with this model are summarized in Table II and the scattering is plotted in Fig. 7 for an energy corresponding to $kR_h=1.90258$. The general variation of the large-angle scattering is the same as for the $\eta$ distribution although the change from one curve to the next is not quite as regular. The average decrease in the large-angle scattering is about 10 percent for an increase in $\lambda$ of 0.04. The corresponding change for the $\eta$ distribution is about 15 percent. The angular distributions intersect at 110°, quite close to the intersection angle of 108° in Fig. 6.

The calculations for the $\eta$ and double-shell densities agree fairly well as regards the general shape of the angular distributions and the rate of change of the large-angle scattering with the fourth moment. There is disagreement, however, in one crucial point. The angular distributions for the same fourth moment produce identical scattering only out to 120°. Beyond this there are differences as large as 7 percent, 5 percent, 10 percent, and 11 percent for fourth moments $\lambda=0.88$, 0.92, 0.96, and 1.00.[34] The validity of a description of electron scattering in terms of even moments is thus no greater than 10 percent for these calculations. This corresponds to an uncertainty in the fourth moment of about 4 percent. Only if the fourth moment of the nuclear charge density differs from that for the homogeneous distribution by much more than 4 percent can the moment interpretation be used.

## VI. EXPERIMENTAL RESULTS BELOW 100 MEV

In Fig. 8 the scattering observed by Lyman, Hanson, and Scott[1] for 15.7-Mev electrons is compared with calculations for the homogeneous charge distribution, which are labeled by the value of $r_0$ in Eq. (1). The experimental points for a particular element do not match any one curve so that estimates of $r_0$ must be made at each angle and then an average taken. For aluminum the finite size effect is very small and the only angles yielding reasonable values are 120° and 150°, for which $r_0=1.2$. The 30° measurement for copper is significantly low; the other points give an average value of $r_0=1.20$. For silver, calculations of the ratio of the actual scattering for $Z=50$ have been used by normalizing the theoretical and experimental values at 30°. A correction has to be made, of course, for the fact that, for the same $kR_h$, $\sigma/\sigma_c$ decreases more rapidly with angle for $Z=50$ than for $Z=47$. The radius for silver is then $r_0=1.13$. Finally the result for gold is $r_0=1.29$. All of these estimates involve an uncertainty of roughly 10 percent due to the standard errors in the data. Thus these determinations are not sufficiently precise to detect any variation with atomic number of the value of $r_0$ needed in Eq. (1). The average radius for the four elements considered is $r_0=1.2$ to within 10

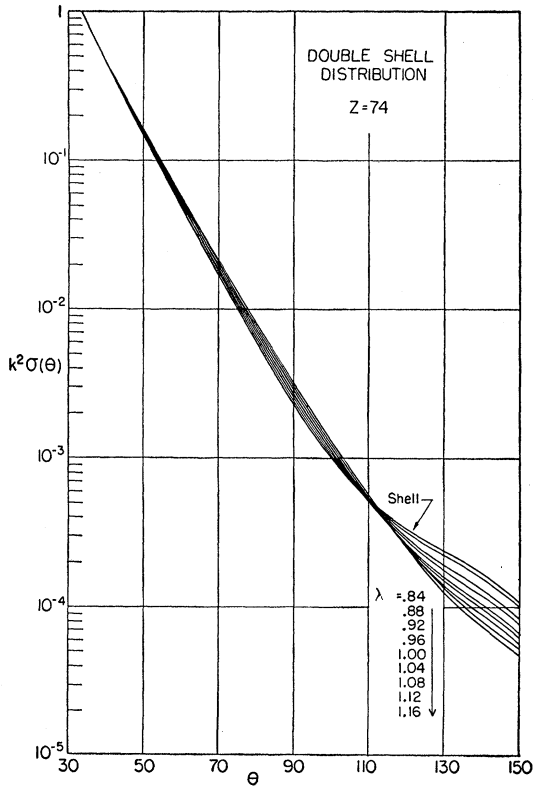


FIG. 7. Angular distributions, $k^2\sigma(\theta)$, for the double shell distribution for $Z=74$ and an energy of 55 Mev. This model consists of two concentric shells of charge $Z_1e$ and $Z_2e$ and radii $r_1$ and $r_2$. In this case $Z_1=50$ and $Z_1+Z_2=74$; $r_1$ and $r_2$ are chosen so that (1) the mean square radius equals that of the homogeneous distribution with $r_0=1.2$, and (2) the fourth moment $\lambda$ ranges from 0.84 to 1.16 in steps of 0.04. These parameters are listed in Table II.

TABLE II. Parameters of the double shell density used to calculate the scattering in Fig. 7. This model consists of two concentric shells of charge $Z_1e$ and $Z_2e$ and radius $r_1$ and $r_2$. The energy is 55 Mev, and $Z=Z_1+Z_2=74$ with $Z_1=50$; $r_1$ and $r_2$ are chosen to give the values of the fourth moment $\lambda$ listed below, keeping the mean square radius equal to that of the homogeneous distribution with $r_0=1.2$.

| $r_1/r_2$ | $r_2/R_h$ | $\lambda$ |
|---|---|---|
| 1.000 | 0.775 | 0.84 |
| 0.803 | 0.888 | 0.88 |
| 0.738 | 0.931 | 0.92 |
| 0.691 | 0.963 | 0.96 |
| 0.654 | 0.989 | 1.00 |
| 0.623 | 1.011 | 1.04 |
| 0.596 | 1.031 | 1.08 |
| 0.576 | 1.049 | 1.12 |
| 0.550 | 1.065 | 1.16 |

[34] No comparison can be made for $\lambda=0.84$ because both models reduce to the simple shell in this case, or for $\lambda>1.00$ because the fourth moment of the $\eta$ distribution is less than or equal to one.

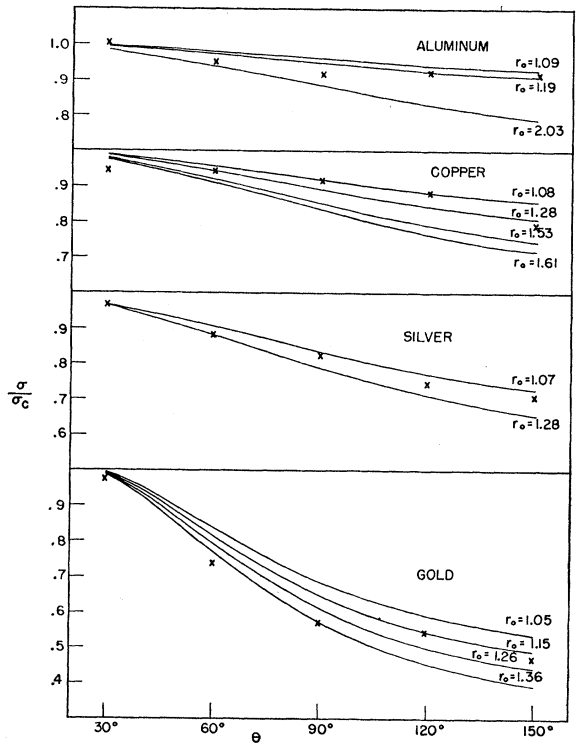


FIG. 8. Comparison of the experimental data at 15.7 Mev with curves for the homogeneous distribution, labeled by the corresponding value of $r_0$. Neglecting observations which cannot be fit by any reasonable choice of $r_0$, the average radius for each element is given by $r_0=1.2$, 1.20, 1.13, and 1.29, for $Z=13$, 29, 50, and 79, respectively. The over-all average is 1.2 with an uncertainty of about 10 percent.

percent, which is somewhat higher than the previous analysis of Bitter and Feshbach.[2]

The experimental values in Fig. 8 are absolute measurements and include an increment of from 5 to 9 percent from the Schwinger formula for radiative corrections.[35] Without these corrections all of the 30° measurements and some of the 60° measurements are too low for any reasonable choice of the radius. Best agreement is expected, however, for just these cases for which the deviations from point scattering are small. One conclusion is that the radiative corrections are not negligible at these energies. If the measurements are not considered as absolute, however, comparison with theory can still be made by normalization of the calculated and observed cross sections *without radiative corrections* at 30°. The average $r_0$ obtained in this way is very close to 1.2, the value obtained with the radiative corrections. The Schwinger formula is valid only for very small $Z$, since it is the Born approximation to the radiative corrections for a point charge. A more accurate examination of the radiative corrections, including the effect of the finite nuclear size, is thus essential. Without it, the 5 or 10 percent corrections of the Schwinger formula represent a limit on the reliability of conclusions from electron scattering.[36]

Some other experiments below 100 Mev are the work of Pidd's group at Michigan. The very precise determination by Pidd, Hammer, and Raka[3] of $\sigma(60°)/\sigma(90°)=7.77\pm0.08$ for $Z=50$ at 34 Mev gives $r_0=1.22\pm0.01$. From relative measurements at 33 and 43 Mev they concluded that the radius of the tungsten nucleus is given by Eq. (1) with $r_0=1.0\pm0.1$. This value is too small, partly because the single-phase-shift analysis[9] is inadequate for tungsten at these energies. Pidd and Hammer[37] have recently obtained new angular distributions (66.25° to 114.5°) for tungsten at 31, 40, and 60 Mev. These are relative measurements with a standard error of about 5 percent. A comparison with the scattering from the homogeneous distribution can be made by normalizing the observed and calculated values at the smallest angle for which measurements were made. No radiative corrections have been included. The values of $r_0$ determined at each energy are $r_0=1.01$, 1.22, and 1.18 at 31, 40, and 60 Mev, respectively. The uncertainty in this analysis is about 10 percent.

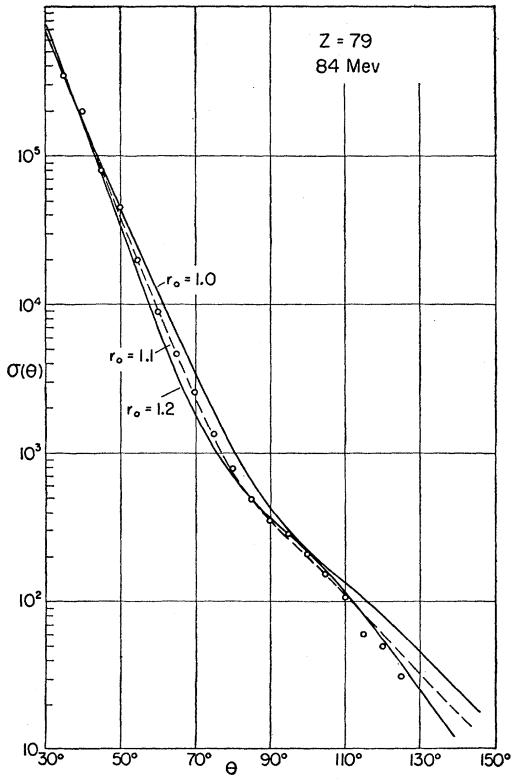


FIG. 9. Comparison of experimental data at 84 Mev for gold with calculations for the homogeneous distribution, labeled by the corresponding value of $r_0$. The curve for $r_0=1.1$ gives the best agreement with the measurements out to 110°.

[35] J. Schwinger, Phys. Rev. **76**, 790 (1949).

[36] R. Hofstadter (reference 4) has pointed out that, for relative measurements at much higher energies, the Schwinger correction is negligible because it changes so slowly with angle compared to the observed cross section.

[37] R. W. Pidd and C. L. Hammer (private communication).

In Fig. 9 we have compared the 84-Mev data for gold obtained at Stanford[5] with calculations for the homogeneous distribution. Here the curves are normalized to the cross section at 35°. For angles less than 110°, good agreement is obtained for a radius given by $r_0=1.10$. The deviation of the three points beyond 110° may be indicative of a fourth moment slightly larger than that for a constant charge density.

In conclusion, the present experimental data for energies below 100 Mev indicate that the mean square radius of the nuclear charge distribution is given by a uniform charge density with $r_0=1.2$. The spread in the experimental data and the uncertainty in the radiative corrections make this determination uncertain by about 10 percent.‡

‡ *Note added in proof.*—Recently the problem of the radiative corrections has received further study by H. Mitter and P. Urban, Acta Phys. Austriaca **8**, 356 (1954); R. Newton, Phys. Rev. **97**, 1162 (1955); H. Suura, Phys. Rev. **98**, 278(A) (1955). Suura's result for the one-photon radiative corrections to high-energy electron scattering is that the leading term (for large momentum transfer and good resolution) of the fractional decrease is given by the Schwinger correction to *all* orders of the Born approximation in the nuclear field.


## ACKNOWLEDGMENTS

The author would like to thank Professor A. O. Hanson for helpful comments on the 15.7-Mev data, and Professor R. W. Pidd for permission to quote his new results prior to publication. The assistance of the Joint Computing Group of M.I.T. is gratefully acknowledged, and in particular the skillful work of Mrs. Evelyn Mack. It is a pleasure to thank Professor Herman Feshbach for suggesting and guiding this work. His continued interest and encouragement is greatly appreciated.


PHYSICAL REVIEW VOLUME 98, NUMBER 5 JUNE 1, 1955

# Nuclear Cross Sections for 1.4-Bev Neutrons*

T. Coor,† D. A. Hill,‡ W. F. Hornyak,§ L. W. Smith, and G. Snow||
*Brookhaven National Laboratory, Upton, New York*

(Received January 11, 1955)

Transmission measurements in good and poor geometry have been performed at the Brookhaven Cosmotron to measure the total and absorption cross sections of several nuclei for neutrons in the Bev energy range. The neutrons are produced by bombarding a Be target with 2.2-Bev protons. The neutron detector requires the incident particle to pass an anticoincidence counter and produce in an aluminum radiator a charged particle that will traverse a fourfold scintillation telescope containing 6 in. of lead. Contribution of neutrons below 800 Mev are believed small. The angular distribution of neutrons from the target is sharply peaked forward with a half-width of 6°.

The integral angular distributions of diffraction scattered neutrons from C, Cu, and Pb are measured by varying the detector geometry. The angular half-width of these distributions indicates a mean effective neutron energy of 1.4±0.2 Bev.

The total cross sections $\sigma_H$ and $\sigma_D-\sigma_H$ are measured by attenuation differences in good geometry of $CH_2-C$ and $D_2O-H_2O$, with the result: $\sigma_H=42.4\pm1.8$ mb, $\sigma_D-\sigma_H=42.2\pm1.8$ mb.

The cross sections of eight elements from Be to U are measured in good and poor geometry, and the following values of the total and absorption cross sections are deduced (in units of millibarns):

| | Be | C | Al | Cu | Sn | Pb | Bi | U |
|---|---|---|---|---|---|---|---|---|
| $\sigma_{\text{total}}$ | 310 | 380 | 700 | 1390 | 2200 | 3210 | 3280 | 3640 |
| $\sigma_{\text{absorption}}$ | 190 | 200 | 410 | 670 | 1160 | 1730 | 1790 | 1890 |

Experimental errors are about 3 percent in $\sigma_{\text{total}}$ and 5 percent in $\sigma_{\text{absorption}}$.

An interpretation of these cross sections is given in terms of optical model parameters for two extreme nuclear density distributions: uniform (radius $R$) and Gaussian $[\rho=\rho_0\exp-(r/a)^2]$. The absorption cross-section data are well fitted with $R=1.28A^{\frac{1}{3}}$ or $a=0.32+0.62A^{\frac{1}{3}}$ in units of $10^{-13}$ cm. A nuclear density distribution intermediate between uniform and Gaussian will make the present results consistent with the recent electromagnetic radii.

## I. INTRODUCTION

THERE has been, in the last few years, a considerable amount of work[1–10] done on the measurement of neutron-nuclei cross sections in the energy range 40–400 Mev. The emphasis has been mainly on transmission measurements in good geometry to measure total cross sections, although in some cases inelastic

* Work performed under contract with the U. S. Atomic Energy Commission.

† Now at Forrestal Research Center, Princeton, New Jersey.

‡ The subject matter of this paper is part of a dissertation presented to the Massachusetts Institute of Technology in partial fulfillment of the degree of Doctor of Philosophy by D. A. Hill. Now at General Electric Laboratory, Schenectady, New York.

§ On leave to the Physics Department, Princeton University, Princeton, New Jersey.

|| On leave to the Physics Department, University of Wisconsin, Madison, Wisconsin.

[1] Cook, McMillan, Peterson, and Sewell, Phys. Rev. **75**, 7 (1949).

[2] Taylor, Pickavance, Cassels, and Randle, Phil. Mag. **42**, 20, 328, 751 (1951).

[3] R. Hildebrand and C. E. Leith, Phys. Rev. **80**, 842 (1950).

[4] R. Hildebrand, University of California Radiation Laboratory Report UCRL-1159, March, 1951 (unpublished).

[5] Bratenahl, Fernbach, Hildebrand, Leith, and Meyer, Phys. Rev. **77**, 597 (1950).

[6] J. DeJuren and N. Knable, Phys. Rev. **77**, 606 (1950).

[7] J. DeJuren, Phys. Rev. **80**, 27 (1950).

[8] Fox, Leith, Wouters, and MacKenzie, Phys. Rev. **80**, 23 (1950).

[9] W. P. Ball, University of California Radiation Laboratory Report UCRL-1938, August 1952 (unpublished).

[10] V. A. Nedzel, Phys. Rev. **94**, 174 (1954).